

A mechanical Duffing oscillator for the undergraduate laboratory

J. E. Berger^{a)} and G. Nunes, Jr.

Department of Physics and Astronomy, Dartmouth College, 6127 Wilder Laboratory, Hanover, New Hampshire 03755-3528

(Received 4 October 1996; accepted 24 February 1997)

The design and construction of a mechanical Duffing oscillator suitable for use in an undergraduate laboratory is described. The oscillator provides a straightforward introduction to nonlinear vibrations and chaotic behavior that is both pedagogically appealing and easily adapted to students at various levels of sophistication. Good agreement is observed between the motion of the oscillator and computer simulations, which provides students with an introduction to the power of mathematical modeling. Period-doubling routes to chaos can be observed both experimentally and numerically. © 1997 American Association of Physics Teachers.

I. INTRODUCTION

The emergence of chaos and nonlinear dynamics as an important topic in physics has led to the development of a wide array of laboratory experiments and lecture demonstrations which exhibit chaotic behavior.¹⁻⁶ Many of these demonstrations, however, remain somewhat unsatisfactory from a pedagogical perspective. The transition from periodic to chaotic behavior may be difficult to observe, or the underlying nonlinearity may be difficult to understand intuitively. Electronic experiments can offer particularly clear demonstrations of such phenomena as period doubling, but may appear only as a “magic black box” to many students. Computer simulations without the benefit of an actual device may reinforce student misperceptions that the physics they are taught has little to say about the real world.

In this paper we describe a mechanical implementation of the Duffing oscillator (inverted pendulum) designed to introduce students at the sophomore or junior level to nonlinear

and chaotic systems. A number of authors have reported on Duffing oscillator implementations which allow both qualitative^{1,6} and quantitative^{5,7} observations of chaotic behavior. In particular, sharp transitions between chaotic and periodic behavior have been reported,⁵ as well as period tripling and amplitude jumps.^{5,7} In this paper, we report on a design that allows both direct observation of the oscillator’s phase space trajectory, and investigations of a period-doubling transition to chaotic behavior. The apparatus can easily be connected to a computer for data acquisition, but is fully functional without one. A particular feature of our implementation is the opportunity for students to make a close quantitative comparison with numerical simulations.

There are several advantages in choosing the Duffing oscillator as an introduction to nonlinear systems. The mathematical equation that describes the motion is easy to derive, and should be accessible to any student who has completed an introductory course in classical mechanics. This deriva-

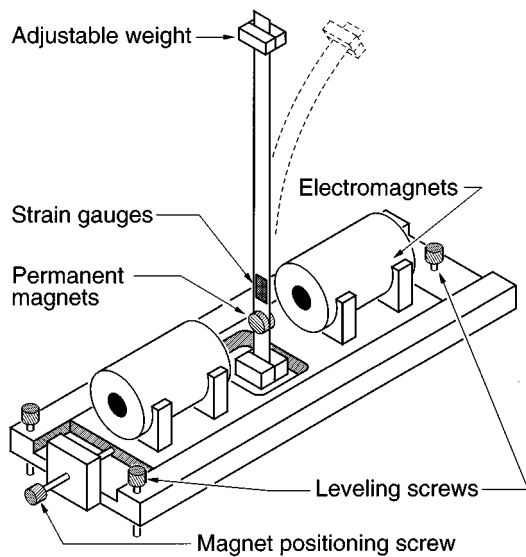


Fig. 1. Schematic diagram of the apparatus. The dashed version of the ruler gives an approximate idea of its shape when it is at one of the two stable equilibrium points.

tion is similar to the more familiar small-angle treatment of the simple pendulum, yet the resulting behavior is wildly different. The time scales for motion of the oscillator itself are slow, which makes the relation between the real-space trajectory and the phase-space trajectory easy to comprehend. Finally, students can numerically integrate the Duffing equation on a personal computer and observe a close correspondence between theory and experiment, which provides them with a dramatic demonstration of the power of mathematically modeling physical systems.

Since our interest lies not only in the apparatus itself, but in how to motivate students to understand the relation between the physical system and its mathematical model, the remainder of this paper is organized in the following fashion: The next section contains an introduction to the Duffing equation, given largely as we introduce our students to it. Section III contains a detailed description of the apparatus. In Sec. IV we discuss the procedure for aligning and running the oscillator, and in Sec. V we show sample results from both the physical oscillator and from numerical simulations. We conclude with a brief summary and discussion.

II. THE DUFFING EQUATION

The Duffing equation was originally derived as a model for describing the forced vibrations of industrial machinery,⁸ and provides a very good approximation of the motion of a damped, driven inverted pendulum with a torsional restoring force. In order to emphasize to the students the similarity between this system and one they are already familiar with, their pre-laboratory problem set first “reminds” them of the equation of motion for a simple pendulum by asking them to derive it, use the small angle approximation, and show that the motion is simple harmonic. They are also asked to show that the natural frequency of the pendulum $\omega_0 = 1$ if time is measured in units of $(l/g)^{1/2}$ (l is the length of the pendulum).

The problem set then asks the students to consider progressively more complicated variations on the pendulum:

They add first a viscous damping term, then a torsional restoring force, and finally invert the pendulum to arrive at the following equation:

$$ml^2\ddot{\theta} = mgl \sin \theta - \alpha\dot{\theta} - k\theta, \quad (1)$$

where m is the mass of the pendulum bob, α is the torsional spring constant, and k is the damping coefficient.

The students are then asked to explore analytically the behavior predicted by Eq. (1) in the limit that $\sin \theta \approx \theta$. In particular, they are asked to show that in this approximation, the equilibrium position $\theta = 0$ is stable only if $mgl < \alpha$, but that the system is predicted to be unconditionally stable, with two equilibrium positions, if $\sin \theta$ is instead approximated as $\theta - \theta^3/6$. The need to add this second term is motivated by pointing out that as the unstable pendulum flops over, the small angle (one-term) approximation will clearly be violated.

In the next step, the students are asked to rewrite the equation of motion with the two-term approximation for $\sin \theta$ if the unit of time is taken to be $(l/g)^{1/2}$. The result, upon inclusion of a driving term, is the Duffing equation for the special case that $a = 1/6$:

$$\ddot{\theta} = -a\theta^3 + b\theta - c\dot{\theta} + f \cos \omega t, \quad (2)$$

where $b = 1 - \alpha/mgl$ and $c = k/mgl$. That Eq. (2) predicts chaotic motion we leave for the students to verify experimentally, both on the computer and in the lab. But as an important step in tying the computer simulations to the real experiment, we ask them to explore the behavior for small deviations from the equilibrium positions at $\theta_0 = \pm(6b)^{1/2}$. In particular, we ask them to express $\theta(t)$ as $\theta_0 + \varphi(t)$ and show that to first order in φ the equation of motion for the oscillator is

$$\ddot{\varphi} + c\dot{\varphi} + 2b\varphi = 0, \quad (3)$$

which again describes simple harmonic motion with a (dimensionless) frequency of

$$\omega_0 = [2b(1 - c^2/8b)]^{1/2} \approx (2b)^{1/2} \quad (4)$$

(weak damping approximation) and a $1/e$ decay time of $2/c$. Therefore, by measuring the frequency and damping for small oscillations about equilibrium, our students can determine the parameters b and c in Eq. (2).

III. APPARATUS

A. Oscillator

A schematic illustration of our mechanical Duffing oscillator is shown in Fig. 1. As in previously reported designs,^{1,5} the oscillator itself consists of a steel strip (in our case, an ordinary 12-in. machinist's rule⁹) rigidly held at the base. A 33-g brass weight can be clamped to the ruler at any height. If the weight is positioned less than 1.5 cm from the top of the ruler, then the vertical equilibrium will be unstable (i.e., $mgl > \alpha$). The weight is composed of two $2.5 \times 1.3 \times 0.6$ -cm brass plates held together with a pair of brass screws. The screws are countersunk and trimmed so that the assembled weight is as nearly as possible a uniform block of metal which surrounds the ruler symmetrically. This apparently minor detail proved essential to the observation of period doubling with the oscillator.

The ruler is driven magnetically. Two 1.3-cm-diam, 0.3-cm-thick neodymium-iron-boron permanent magnets¹⁰ are

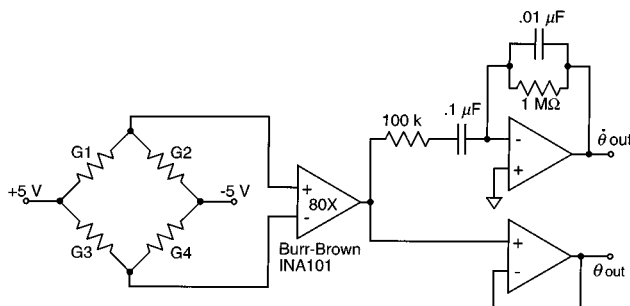


Fig. 2. Schematic diagram of the electronic readout. For simplicity, variable gain is provided by the oscilloscope or x - y recorder, rather than by the circuit. The strain gauge elements G1–4 are mounted on the ruler, and have a nominal resistance of $1\text{ k}\Omega$.

clamped to the ruler by their own field 2.5 cm above the base. A sinusoidal driving force is applied to these permanent magnets by a pair of electromagnets consisting of approximately 2300 turns of 0.04-cm-diam copper magnet wire wound on a 1.3-cm-diam ferrite core.¹¹ The magnets were wound on a lathe with no particular attempt made to close-pack the windings. A pair of 3.5-cm-diam plastic disks glued 4 cm apart onto each core served to confine the winding and ensure a uniform cross section along the length of the magnets. The total resistance of the two magnets in series is $70\text{ }\Omega$, so that when driven with 10 V from our signal generator ($50\text{ }\Omega$ output impedance), they generate a peak field of 60 G. The distance between the magnet pole pieces and the permanent magnets on the ruler is approximately 3 cm. This distance was chosen so that the force exerted on the ruler is largely independent of the bending of the ruler. If the electromagnets are too close to the ruler, then as the ruler bends toward one magnet, it becomes even more strongly attracted to that magnet. The amplitude of the driving term then becomes a function of the bending angle, and the resulting motion is not described by the Duffing equation.

In order to allow the electromagnets to be adjusted so that they exert a symmetric force on the ruler, they are rigidly mounted to a separate plate which in turn is placed in a wide groove in the base plate that holds the ruler. The magnet plate can be positioned within this groove using a pair of fine adjustment screws.¹² (The alignment procedure for the oscillator is described below.) The groove ensures that the travel of the magnets is confined to the plane of the ruler's bending motion.

The deflection of the ruler is measured with a set of four strain gauges (two matched pairs¹³) mounted 5 cm above the base. The matched pairs are epoxied on opposite sides of the ruler, and are wired as a Wheatstone bridge. In order to keep unwanted forces on the oscillator to a minimum, the connections between the strain gauges and the electronics are made with 0.08-mm-diam phosphor bronze wire.

The base plate which supports the oscillator can be leveled with a set of three 0.3-mm pitch (80 threads per in.) screws (identical to those used to position the electromagnets). The leveling screws bear on a set of steel inserts in a second aluminum plate which is fastened to the lab bench. The two plates are kept in rigid contact by a pair of stiff springs.

Much to our surprise, air currents proved to be a major limitation to the stability and reproducibility of the oscillator. A simple Plexiglas™ box with no bottom and a removable lid can be placed over the oscillator to shield out these per-

turbations. The removable lid allows minor adjustments to the oscillator without risk of seriously upsetting it.

B. Electronics

The electronics setup used to display the motion of the oscillator is extremely simple, and allows the direct display of a phase space plot ($\dot{\theta}$ vs θ) on a storage oscilloscope or x - y recorder. The four strain gauges are wired into a Wheatstone bridge, as illustrated in Fig. 2. Gauges G1 and G4 are a matched pair on one side of the ruler, while G2 and G3 are a matched pair on the other. The nominal resistance of each gauge is $1\text{ k}\Omega$. The bridge is excited with 10 V_{dc} and the out-of-balance signal is differentially amplified¹⁴ and fed to two separate output stages. One of these stages is simply a buffer that provides an output proportional to θ , the bending angle of the ruler, and is used to drive the x channel of an oscilloscope or pen recorder. The other stage is a differentiator which provides an output proportional to $\dot{\theta}$ and is used to drive the y channel on the display. The op-amps can be of any convenient type (we used OP-07 amplifiers¹⁵ which have a very low output offset voltage). Under normal operation, both signals span about 2 V. We use the oscilloscope controls to provide variable gain and to null out the small offset in the θ signal due to imperfect matching of the strain gauges.

Since the ruler bends along its whole length, relating the output voltage to the "angle" θ requires some care. Following Duchesne *et al.*⁵ we define θ to be the angle between a tangent to the free end of the ruler, and the direction of gravity. With this definition, the output voltage is a linear function of θ (to within 2%) over $\pm 0.4\text{ rad}$ ($\pm 23\text{ deg}$). All of the motions reported here fall within this linear-output range.

The motion of the oscillator is driven by connecting the electromagnets directly to the output of a synthesized signal generator.¹⁶ The use of a generator with high resolution and high stability in both amplitude and frequency is absolutely essential. We observed that regions of chaotic and periodic behavior could be separated by as little as 10^{-3} Hz or 10^{-3} V .

IV. PROCEDURE

Although it is relatively easy to find regions of chaotic behavior with the oscillator, observing a period-doubling cascade requires careful alignment. Our procedure therefore begins with the adjustment of the leveling screws so that the ruler (with the weight removed) is parallel to a hanging plumb line. Then, with the center of the weight positioned $\sim 10\text{ mm}$ from the top of the ruler, further fine adjustments are made so that when released from a vertical position, the ruler bends to either side with equal preference.

The final step in the alignment procedure involves adjusting the electromagnets so that their effect on the ruler is symmetric. We set the oscillator into large amplitude oscillations, determine the period, and set the signal generator to maximum amplitude at the corresponding frequency ($\sim 0.15\text{ Hz}$). The resulting phase-space orbit has a characteristic shape that looks a bit like the outline of a boot. Any asymmetries in this shape (in which the "heel" can be differentiated from the "toe") are removed by carefully adjusting the position of the electromagnet assembly.

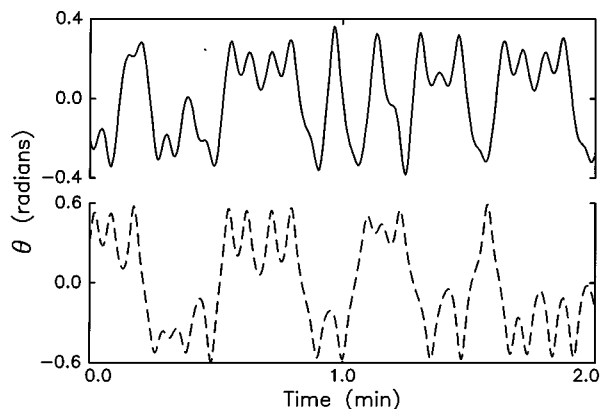


Fig. 3. A comparison of θ vs t from the actual oscillator (upper trace, solid line) and a computer simulation (lower trace, dashed line) in the chaotic regime. The experimental trace is 1.6 V peak-to-peak, and has been converted to radians. The Duffing equation parameters were, for the experiment and simulation, respectively: $b=0.027$ and 0.03 , $c=0.013$ and 0.02 , and drive frequency $\omega/2\pi=0.200$ and 0.19 Hz. The dimensionless time variable in the simulation was converted to seconds using $(l/g)^{1/2}=0.17$ s, as discussed in the text. The drive amplitude in the experiment was 6 V and in the simulation was 0.003.

As an aid in making a meaningful comparison between laboratory observation and computer calculation, at this point our written instructions ask the students to shut off the drive and measure both the natural frequency and damping of the ruler for small oscillations about one of the two equilibrium positions. For our apparatus, a natural frequency of 0.22 Hz and a $1/e$ time of 27 s are typical. These correspond to $b=0.027$ and $c=0.013$ in Eq. (2), respectively, with $(l/g)^{1/2}=0.17$ s. The quantity $c^2/8b=0.001$, so the weak damping approximation made in Eq. (4) is well justified.

Once the oscillator has been aligned, observing chaotic behavior is straightforward. We typically operate at a fixed drive frequency of 0.200 Hz (10% below the natural frequency for small oscillations). A quick binary search in drive voltage easily locates the boundary between periodic and chaotic motion to within a few tenths of a volt. Observing a period-doubling cascade requires a much more patient sweep in drive voltage toward the chaotic regime. In all cases, we re-start the oscillator with the same initial conditions following any change in the drive voltage. Our procedure is to disconnect the drive and manually bring the pendulum to rest in one of its stable equilibrium positions. The drive can be monitored on an oscilloscope, and because of its low frequency, manually reconnected at the same point in its cycle, so that the oscillator starts with as near as possible the same set of initial conditions (position, velocity, and phase with respect to the drive) after each adjustment. Simply detaching and re-attaching the cable from the output of the signal generator provides a sufficiently fast "switch." Once the oscillator has been re-started, several minutes are required for the initial transients to decay and for the system to settle into either periodic or chaotic motion.

V. RESULTS AND DISCUSSION

The Duffing equation has been extensively studied through both analytical and numerical investigations.¹⁷⁻²¹ Our purpose here is to focus on the experiment and the opportunity it offers students to observe the same complex be-

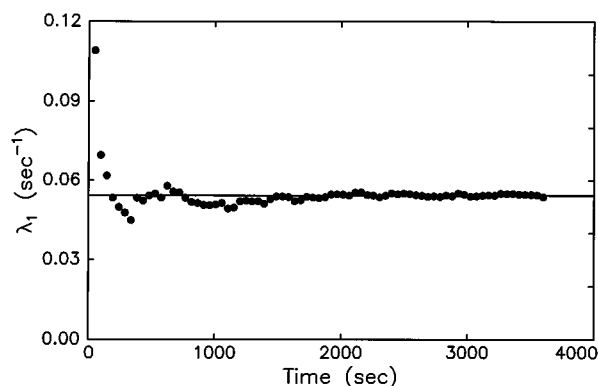


Fig. 4. Convergence of the largest positive Lyapunov exponent (λ_1) calculated using the methods of Ref. 25. A series of 7500 measurements of $\theta(t)$ at 0.48-s intervals was embedded in three dimensions by taking the triple $(\theta(t), \theta(t+\tau), \theta(t+2\tau))$ to be the x, y, z coordinates of a point on the attractor. τ was taken to be 14.4 s, and the divergence of adjacent points on the attractor was followed for 48 s. For details on the calculation, see Ref. 25 and, e.g., Ref. 23.

havior in both a real system and in a mathematical model. Figure 3 shows a comparison of the θ vs t behavior in the chaotic regime for both the actual oscillator (upper trace, solid line) and for a numerical simulation (dashed line). The experimental data were acquired with a personal computer and digitizing interface.²² The simulation uses a fourth-order Runge-Kutta algorithm (adapted from Ref. 23) to numerically integrate Eq. (2) on a personal computer. The parameter b was set equal to 0.03 in order to closely mimic the natural frequency of the apparatus, and the drive frequency

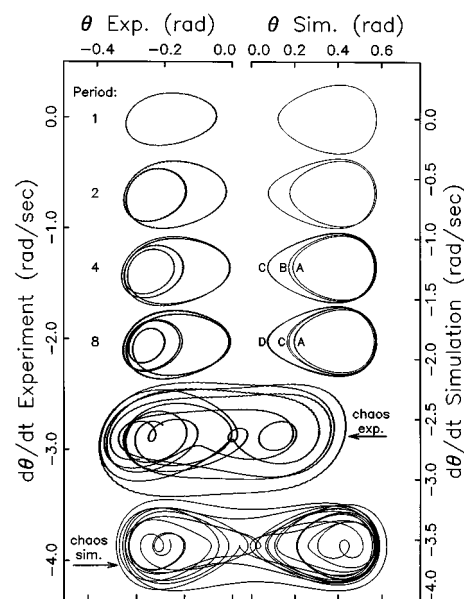


Fig. 5. A comparison of period-doubling cascades to chaos observed in the experiment (left-hand side) and simulation (right-hand side). The parameters b , c , and $\omega/2\pi$ for the simulation are the same as in Fig. 3. In the period 8 plot, the label B for the trajectory loop between loops A and C has been omitted for clarity. The experimental drive amplitudes are period 1: 4.7 V, period 2: 4.9 V, period 4: 5.1 V, period 8: 5.1 V, chaos: 5.2 V. The simulation drive amplitudes are period 1: 0.002, period 2: 0.0022, period 4: 0.002 245, period 8, 0.002 247, chaos: 0.003. All plots beyond period 1 have been offset for clarity.

was set to 0.2 [corresponding to 0.19 Hz for $(l/g)^{1/2} = 0.17$ s]. We found, however, that the parameter c had to be set to 0.02 to provide adequate damping, about 55% above our measured value. The amplitude of the drive signal in the experiment was set to 5 V, while the drive parameter f in the simulation was 0.003. (We made no effort to directly relate the drive amplitude in the simulation to the drive voltage in the experiment.) The amplitudes of the experimental signal (0.4 rad or 1.6 V peak-to-peak) and the simulated motion (0.6 rad peak-to-peak) are reasonably similar. The correspondence in the time domain is even stronger. Once the time axis for the simulated data has been converted to seconds [using $(l/g)^{1/2} = 0.17$ s], the experimental and numerical signals can be seen to have remarkably similar characteristic time scales. The initial conditions in the simulation were the same as in the experiment: The oscillator was started from rest in one of its potential minima. The close correspondence between the parameters of the simulation and the measured parameters of the oscillator show that the predictions of the simulation are quantitatively as well as qualitatively correct.

Determining the true nature of the behavior illustrated in Fig. 3 requires some care. What appears inchoate to the unaided eye may or may not be truly chaotic. While there are a number of methods available to test for the presence of true chaos, determining that the system has at least one positive Lyapunov exponent is considered definitive.^{23,24} Other methods, e.g., power spectra can be used, and may be more appropriate for students who are not yet comfortable with the idea of phase space. (See Ref. 5 for a good discussion of the advantage of using the power spectrum, as well as advice on how to overcome some of the difficulties in determining the spectrum correctly). Figure 4 shows the convergence of the largest Lyapunov exponent λ_1 determined from an hour-long run of the oscillator. The motion was digitized at 2.08 Hz, and the Lyapunov exponent was calculated (using the method of Wolf *et al.*²⁵) from the resulting 7500 point record of $\theta(t)$.

As mentioned in the Introduction, a particularly appealing aspect of the Duffing oscillator is the possibility of observing a period-doubling cascade in a mechanical system. Figure 5 shows a comparison of a cascade showing periods 1, 2, 4, and 8 in both the mechanical system and the computer simulation. Both sets of data are plotted as $\dot{\theta}$ (along the vertical axis) vs θ (along the horizontal axis). Only the limit cycles are shown, the initial transient behavior in both cases having been discarded. The experimental data were taken with a standard x - y plotter. The left-hand set of axes gives the correct scale for the experimental data, while the right-hand axes apply to the simulation. The plots are offset vertically for clarity. The plots at the bottom of the figure show chaotic behavior in both systems. There is a small amount of higher frequency noise (~ 15 Hz) visible in the experimental data which comes from transverse vibrations of the ruler. The load imposed by the weight is close to that required to buckle the ruler, so this transverse mode is always slightly excited. (These oscillations were filtered out by the digitizer used to acquire the data in Fig. 3.)

The interpretation of the “eggs” in Fig. 5 is straightforward (particularly for a student able to simultaneously watch the oscillator, a phase space plot, and trace of θ as a function of time). Since the oscillations are not strictly sinusoidal, the phase plot for simple periodic motion is not quite a circle. When the period of the motion doubles, every other peak in

$\theta(t)$ has a reduced height, which results in the “egg” developing a “yolk.”²⁶ When the period doubles again (to period 4), there are now three different peak heights in $\theta(t)$. If the loops in the period 4 plot are labeled A , B , and C from innermost to outermost, the oscillator traverses the attractor in the sequence $ACBCACBC\cdots$. The motion in the case of period 8 is $ADBDADCDADBDADCD\cdots$, where A represents the innermost loop and D represents the outermost.

The data in Fig. 5, while showing what is possible with the oscillator, also point out some of its limitations. Note that the period 4 and period 8 data were taken at the same drive voltage. The characteristics of the oscillator are observed to drift with time, probably as a result of thermal changes or mechanical creep. The period 4 and period 8 data were taken several hours apart, so that the boundary between high order periodic and chaotic motion had shifted. The extra structure in the experimental limit cycles (as compared to the simulation) is due, we believe, to residual asymmetry in the adjustment of the oscillator. Unless considerable effort (primarily trial and error) is made to eliminate such asymmetry, higher order periodicity (4 and 8) cannot be observed. Rather, the motion doubles to period 2, remains at period 2 through a broad range of drive voltage (~ 0.5 V), and then goes directly to chaos. As a result, period-doubling cascades are only likely to be observed by more advanced (and patient) students. Periodic versus chaotic behavior, however, can readily be observed in a laboratory exercise at the introductory level.

VI. CONCLUSION

We have presented the design for a nonlinear chaotic oscillator, and shown that its behavior corresponds to the predictions of a numerical simulation—both qualitatively and quantitatively. The apparatus can be used in conjunction with a computerized data acquisition system, or with a simple analog x - y recorder. Doubling to period 2 and chaotic motion are readily observed, and with care, period-doubling cascades can be seen. The true chaotic nature of the motion can be verified by finding a positive Lyapunov exponent. The apparatus thus allows students to observe a direct relation between the real and numerical worlds and to discover the power of mathematical modeling.

ACKNOWLEDGMENTS

The authors are grateful to B. McNamara at Reed College for helpful discussions about construction of the oscillator. JEB acknowledges the support of the Dartmouth College Class of 1939 Presidential Scholars Fund. GN acknowledges the support of an Alfred P. Sloan Research Fellowship.

^{a)}Current address: Physics Department, Brown University, Providence, Rhode Island.

¹K. Briggs, “Simple experiments in chaotic dynamics,” *Am. J. Phys.* **55**, 1083–1089 (1987).

²J. A. Blackburn, S. Vik, B. Wu, and H. J. T. Smith, “Driven pendulum for studying chaos,” *Rev. Sci. Instrum.* **60**, 422–426 (1989).

³M. J. Ballico, M. L. Sawley, and F. Skiff, “The bipolar motor: A simple demonstration of deterministic chaos,” *Am. J. Phys.* **58**, 58–61 (1990).

⁴A. Ojha, S. Moon, B. Hoeling, and P. B. Siegel, “Measurements of the transient motion of a simple nonlinear system,” *Am. J. Phys.* **59**, 614–619 (1991).

⁵B. Duchesne, C. W. Fischer, C. G. Gray, and K. R. Jeffrey, “Chaos in the motion of an inverted pendulum: An undergraduate laboratory experiment,” *Am. J. Phys.* **59**, 987–992 (1991).

- ⁶R. D. Peters, "Chaotic pendulum based on torsion and gravity in opposition," *Am. J. Phys.* **63** (12), 1128–1136 (1995).
- ⁷N. Alessi, C. W. Fischer, and C. G. Gray, "Measurement of amplitude jumps and hysteresis in a driven inverted pendulum," *Am. J. Phys.* **60**, 755–756 (1992).
- ⁸G. Duffing, *Erzwungene Schwingungen bei veränderlicher Eigenfrequenz und ihre technische Bedeutung* (Friedr. Vieweg & Sohn, Braunschweig, 1918).
- ⁹L. S. Starrett Co., Athol, MA, No. C305R.
- ¹⁰McMaster–Carr, New Brunswick, NJ, stock No. 5862K53.
- ¹¹McMaster–Carr, New Brunswick, NJ, stock No. 8495K85.
- ¹²Thor Labs, Newton, NJ, stock No. FAS150.
- ¹³Omega Engineering, Stamford, CT, stock No. SG-3/1000-DY41.
- ¹⁴Model No: INA101, Burr–Brown Corp., Tucson, AZ. Available from, e.g., Digi-Key Corp., Thief River Falls, MN.
- ¹⁵Analog Devices, Norwood, MA. Available from, e.g., Allied Electronics, Forth Worth, TX.
- ¹⁶Hewlett–Packard model No. 3325A. This generator was chosen for convenience. Any signal source with resolution and reproducibility of 1 mHz and 1 mV would be sufficient. Because the oscillator acts as a low pass filter with a corner frequency at about 0.2 Hz, requirements on harmonic distortion are more modest.
- ¹⁷N. Takimoto and H. Yamashida, "The variational approach to the theory of subharmonic bifurcations," *Physica D* **26**, 251–276 (1987).
- ¹⁸Y. Ueda, H. Nakamima, T. Hikihara, and H. B. Stewart, "Forced two well potential Duffing oscillator," in *Dynamical Approaches to Nonlinear Problems in Systems and Circuits*, edited by F. M. A. Salam and M. Levi (SIAM, Philadelphia, 1988), pp. 128–137.
- ¹⁹J. Awrejcewicz, "Numerical versus analytical conditions for chaos, using the example of the duffing oscillator," *J. Phys. Soc. Jpn.* **60**, 785–788 (1991).
- ²⁰S. De Souza-Machado, R. W. Rollins, D. T. Jacobs, and J. L. Hartman, "Studying chaotic systems using microcomputer simulations and Lyapunov exponents," *Am. J. Phys.* **58**, 321–329 (1990).
- ²¹C. L. Olson and M. G. Olsson, "Dynamical symmetry breaking and chaos in Duffing's equation," *Am. J. Phys.* **59**, 907–911 (1991).
- ²²MacScope, Thornton Associates, Boston, MA.
- ²³G. L. Baker and J. P. Gollub, *Chaotic Dynamics* (Cambridge U.P., Cambridge, 1990).
- ²⁴E. Ott, *Chaos in Dynamical Systems* (Cambridge U.P., Cambridge, 1993).
- ²⁵A. Wolf, J. B. Swift, H. L. Swinney, and J. A. Vastano, "Determining Lyapunov exponents from a time series," *Physica D* **16**, 285–317 (1985).
- ²⁶Thanks to M. D. Sturge for this biological analogy.